Çukurova Üniversitesi
Mühendislik Fakültesi Dergisi
Çukurova University
Journal of the Faculty of Engineering
ISSN: 2757-9255 CİLT/VOLUME: 39 SAYI/ISSUE: 3 EYLÜL/SEPTEMBER 2024

Optimal Design and Analysis of High-Frequency Isolation Transformer for Switched-Mode Power Converters

Abdurrahman YAVUZDEĞER [1,a], **Burak ESENBOĞA** [2,b], **Tuğçe DEMİRDELEN** [2,c]

[1]*Adana Alparslan Türkeş Science and Technology University, Faculty of Engineering, Department of Energy Systems Engineering, Adana, Türkiye*
[2]*Adana Alparslan Türkeş Science and Technology University, Faculty of Engineering, Department of Electrical and Electronics Engineering, Adana Türkiye*

[a]***ORCID**: 0000-0001-8058-4672; [b]**ORCID**: 0000-0002-7777-259X; [c]**ORCID**: 0000-0002-1602-7262*

Article Info
Received : 21.02.2024
Accepted : 27.09.2024
DOI: 10.21605/cukurovaumfd.1559912

Corresponding Author
Abdurrahman YAVUZDEĞER
ayavuzdeger@atu.edu.tr

Keywords
High-frequency transformer
Modeling
Electromagnetic
ANSYS/Maxwell
Loss analysis
Flyback

How to cite: *YAVUZDEĞER, A., ESENBOĞA, B., DEMİRDELEN, T., (2024). Optimal Design and Analysis of High-Frequency Isolation Transformer for Switched-Mode Power Converters. Cukurova University, Journal of the Faculty of Engineering, 39(3), 585-598.*

ABSTRACT
High-frequency (HF) transformers have gained great interest in recent years due to the advent of powerful soft magnetic materials with low core loss in semiconductor power switches. Also, the optimal design of the HF transformer is a significant issue for high-performance energy conversion systems. In this paper, a 40W 50/12.5/25 V universal input and two output discontinuous-conduction mode (DCM) flyback transformer is designed by using mathematical calculations and analyzed via 3D ANSYS/Maxwell simulation including electromagnetic and loss analysis. It is shown that the simulation results accounting for hysteresis losses, eddy current losses, copper losses, and magnetic flux density determine the accuracy of the mathematical model calculation. Analyzes are performed at 100 kHz frequency levels. Results obtained will include core magnetic flux density, core/copper losses, leakage/magnetizing inductances, windings parasitic capacitances, input/output voltage, current values, and all design parameters. Finally, the proposed HF transformer's overall efficiency is calculated and presented. Significantly, the HF transformer achieves 97.8% efficiency thanks to the transformer's core and coil selection, B-H and B-P characteristics, one-to-one dimension design, and mesh operation. The dynamic and mathematical results of the designed transformer demonstrate the design and efficiency success.

Anahtarlamalı Güç Dönüştürücüleri için Yüksek Frekanslı İzolasyon Transformatörünün Optimum Tasarımı ve Analizi

Makale Bilgileri
Geliş : 21.02.2024
Kabul : 27.09.2024
DOI: 10.21605/cukurovaumfd.1559912

Sorumlu Yazar
Abdurrahman YAVUZDEĞER
ayavuzdeger@atu.edu.tr

Anahtar Kelimeler
Yüksek frekans transformatör
Modelleme
Elektromanyetik
ANSYS/Maxwell
Kayıp analizi
Geri dönüşlü

Atıf şekli: *YAVUZDEĞER, A., ESENBOĞA, B., DEMİRDELEN, T., (2024). Optimal Design and Analysis of High-Frequency Isolation Transformer for Switched-Mode Power Converters. Cukurova University, Journal of the Faculty of Engineering, 39(3), 585-598.*

ÖZ
Yüksek frekanslı (YF) transformatörler yarı iletken güç anahtarlarında düşük çekirdek kaybına sahip güçlü yumuşak manyetik malzemelerin ortaya çıkması nedeniyle son yıllarda büyük ilgi görmektedir. Ayrıca YF transformatörünün optimal tasarımı, yüksek performanslı enerji dönüşüm sistemleri için önemli bir konudur. Bu makalede, 40W 50/12.5/25 V tek girişli ve iki çıkışlı süreksiz iletim modlu (SİM) bir geri dönüş transformatörü matematiksel hesaplamalar kullanılarak tasarlanmış ve elektromanyetik ve kayıp analizini içeren 3B ANSYS/Maxwell simülasyonu ile analiz edilmiştir. Histerezis kayıplarını, girdap akımlarını, bakır kayıplarını ve manyetik akı yoğunluğunu hesaba katan simülasyon sonuçlarının matematiksel model hesaplamasının doğruluğunu belirlediği göstermektedir. Analizler 100 kHz frekans seviyelerinde gerçekleştirilir. Elde edilen sonuçlar çekirdek manyetik akı yoğunluğunu, çekirdek/bakır kayıplarını, sızıntı/mıknatıslama endüktanslarını, sargıların parazit kapasitanslarını, giriş/çıkış voltajını, akım değerlerini ve tüm tasarım parametrelerini içerecektir. Son olarak önerilen YF transformatörünün genel verimliliği hesaplanmış ve sunulmuştur. YF transformatörünün, transformatörün çekirdek ve bobin seçimi, B-H ve B-P özellikleri, birebir boyut tasarımı ve ağ çalışması sayesinde %97,8 verim elde etmesi dikkate değerdir. Tasarlanan transformatörün dinamik ve matematiksel sonuçları, tasarım ve verimlilik başarısını ortaya koymaktadır.

1. INTRODUCTION

Transformers are one of the main components of the electrical energy transmission and distribution system. Thanks to transformers, electricity transmission, and distribution have become easier and more useful.

In recent times, there has been a notable rise in the variety of transformers employed in small and medium-scale power applications. Among these, high-frequency transformers stand out as one of the most crucial types [1]. These transformers are widely used in the field of power electronics, electric vehicle and renewable energy applications [2-8]. These transformers are preferred in power electronics in terms of reliability, stability, and quality. They are also very useful in terms of size, cost, and efficiency. They are generally small in size. Therefore, it is both less costly and more convenient for power electronics. Researchers have done a lot of work to minimize core loss for high-frequency transformers and optimize properties such as efficiency and cost [9-12].

It is investigated the effect of wire type and interleaved winding structure on the electric field distribution of medium frequency transformers using the 2D finite element method (FEM). The study presents the six different forms of non-interleaved windings with various wire types. The maximum electric field intensities are measured and compared [13]. A high-frequency transformer (HFT) is of great importance in obtaining a high-efficiency Solid State Transformer (SST). And for this, a multi-purpose optimization algorithm has been developed that minimizes the core volume and minimizes the total losses that may occur in the transformer, and the total cost of the HFT [14]. An HFT is used for DC/DC conversion. The transformer has dry-cast windings and is designed for DC system voltages up to 50kV. It has been observed that the individual cast LV and HV windings provide good efficiency with insulation size and performance. The AC insulation test was carried out for 70 kV and the LI voltage test for 150 kV. At these voltages, careful grading down to the PD test voltage is important, to prevent discharge in air. In addition, careful insulation of the HV terminals near the grounded components of the HFT is also required [15].

It is presented different core and coil materials under the variable medium frequencies [16]. In a frequency range of up to 10kHz, a performance factor is used to determine the acceptability of each material. From the result of these evaluations, it has been shown that amorphous and nanocrystalline materials perform better in high-frequency applications above 1 kHz, and amorphous materials can outperform SiFe materials due to losses at low frequencies (60-200 Hz). High-frequency transformers (HFT) are used in a lot of modern-day applications. Ordinary winding topology is being used in most of these high-frequency transformers and because of that, the magnetic core saturates without guaranteeing the maximum power transfer (DWT). To get over this issue, it is introduced a new distributed winding topology. To apply this DWT the magnetic core should be changed in terms of its shape and size to optimize. It is proven that DWT-based HFT transfers %48.37 more power than the regular one [17]. Because of the lack of freedom and difficulty in obtaining the optimal solution fast and correctly the traditional converter is not optimal. To overcome this issue an HFT design that uses the ALO algorithm is introduced [18]. By using different conductors and winding arrangements on an HFT, the skin effect can be studied. AC winding resistance increases and the leakage inductance decreases with the skin effect as the frequency goes higher. In wire conductors, the shape of the wires can affect the parasitic and loss behavior. Skin effects behavior in the conductor changes with the shape of the wires as well. This study shows that by changing the square shape to a circular shape the winding loss and the leakage inductance increase up to 2 times and 1.2 times respectively [19]. It is determined the best high-frequency transformer design for maximum performance. Magnetic core material, precisely estimating the core loss, and experimental methodologies for core loss measurement are discussed. In addition, the performance of a transformer is determined by winding loss or copper loss, leakage inductance, leakage resistance, stray capacitance, and thermal analysis. All requirements that are described, are critical to optimize the design of a high-frequency transformer to get high power density and efficiency [20]. It is examined and analyzed high-frequency transformer leakage inductances and parasitic capacitances for different windings and structures. It is. used the finite element method for the analysis of these transformers. These results, looking at the relationship and balance between leakage inductance and parasitic capacitance values, have helped in classifying and designing the structure of this transformer [21]. It is mentioned the overall effect of interleaving on leakage induction, a general method used to reduce induction and may also cause increased parasitic capacitance. One of the parts is the plane transformation applications in the high voltage area and the design of the exchange between all interference. It suggests the partially reserved transformer structure improved for high-voltage and high-frequency multiple outputs [22]. It is conducted to design a high-frequency high voltage transformer. Core

selection, losses and thermal model for a high-frequency transformer in LLC resonant converters are studied. 3F4 ferrite core for the high-frequency transformer, the design is realized by using E38/9/15 core. This high-frequency transformer design is installed in an LLC resonant converter at 800 V [23]. A medium frequency transformers model with a complete analytical steady- state thermal network has been proposed and experimentally verified using finite element technique analysis. The similarities between the FEM model and analytical model show that the model built is extremely accurate. Due to the low quality of empirical natural air convection models and their restricted applicability on the specified geometrical details, there were several issues with the calculated and measured temperatures. Although analytical models are quick to implement, they must be rigorously connected with experimental data [24]. It is suggested a novel data-driven technique for extracting FEM simulation data of high-frequency transformers featuring litz-wire windings. By homogenizing these windings, computational expenses are significantly diminished. The findings show that the double 2-D FEM model introduced, accounting for inner and outer core window length factors, adeptly captures the three-dimensional nature of leakage inductance within high-frequency transformers [25]. It is introduced a design for a multi-winding (HFT) aimed at a multiport unified charge converter. It includes the development of a loss model and provides a step-by-step procedure for designing the multi-winding transformer [26]. Another study presents the development of a model for HFT windings. This model enables the calculation of voltage distribution along the winding and the identification of its resonance frequencies [27].

Upon reviewing the existing literature, it becomes evident that high-frequency (HF) transformers have been extensively studied and applied across various power applications. However, a noticeable gap exists concerning detailed design methodologies and electromagnetic analyses specifically tailored for HF transformers. While numerous studies are exploring their functionalities and applications, there's a scarcity of in-depth examinations focusing on the intricate design and electromagnetic behaviors inherent to HF transformers. This void underscores the need for further research and analysis in this specialized domain to advance the understanding and optimization of HF transformer performance. Thus, the main focus of this study is;

- to calculate the design parameters and core losses of the HF transformer thanks to the mathematical model and realist simulation study.
- to present the more efficient HF transformer model.
- to create a 3D model and realize the electromagnetic analysis with ANSYS/Maxwell.
- to verify the effectiveness of the mathematical model with the electromagnetic analysis.

In this paper, the mathematical model of a HF transformer is discussed in detail. All parameters such as power, weight and electromagnetic calculations are given thanks to the mathematical model. Also, the proposed HF transformer is modeled and analyzed via ANSYS/Maxwell program. Electromagnetic analysis results present the losses, magnetic flux distribution of the core and magnetic field distribution of the transformer. Thus, the efficiency and performance analysis of the HF transformer is performed before the transformer is produced.

2. MATERIAL AND METHOD

2.1. Structure Analysis of High-Frequency Transformers

A transformer is an electrical machine that transfers energy from one electrical circuit to the next or numerous circuits. High-frequency transformers are one of the sorts, with frequencies ranging from 10 kHz to 1MHz. There are numerous advantages to using a higher frequency for this high-frequency transformer. The transformer's size is the first of these. The smaller the transformer is for any power rating, the greater the frequency. Second, because the transformer is smaller, less copper wire is required, which reduces losses and helps the high-frequency transformer to be more efficient and operate. The use of Litz wire in high-frequency transformers is an important factor in reducing the skin effect. Because of this to lessen the skin effect, Litz wire is preferred. High-frequency transformers are classified into three types as flyback transformer, push-pull transformer and forward transformer.

A flyback transformer is a hollow core inductor with a combined inductor. Once the input voltage is supplied to the primary winding throughout each cycle, energy is contained in the cavity of the core. To energize the load, this voltage is subsequently transmitted to the secondary winding. Voltage transformation

and circuit isolation are provided by flyback converters shown in Figure 1. The transformer isolation or turn-ratio voltage transformation is provided by the flyback topology, which is based on a buck-boost topology.

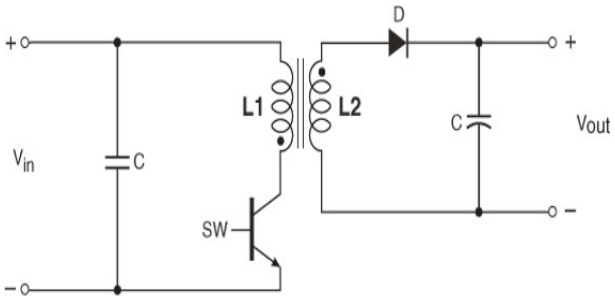

Figure 1. Typical flyback converter schematic

A switch controls the primary winding of the flyback transformer. The main inductance causes the current to build up in a ramp when the switch is turned on. The creation of secondary current, which would eventually oppose the primary current ramp, is prevented by an integrated diode linked in series with the secondary winding. The current in the main decreases to zero when the switch is switched off. As the magnetic field in the core shrinks, the energy contained in it is released to the secondary. The output winding voltage rises rapidly (typically less than a microsecond) until it is restricted by the load circumstances.

Flyback transformers basically work in two modes. The secondary current will never reach zero only when the FET (Field Effect Transistor) SW return is turned on again until all of its energy has been transferred to the secondary. A continuous transmission mode (CCM) waveform is depicted in Figure 2.

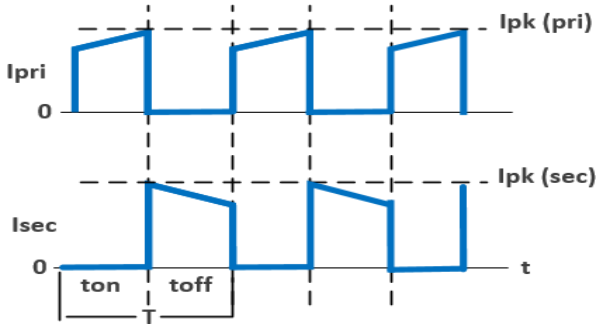

Figure 2. Continuous current mode (CCM) flyback current waveforms

If the stored return energy discharges fully to the secondary before the FET comes on once again, the secondary current hits zero before the period expires, resulting in a "idle time" (tde) during the cycle. This kind of transmission is known as discontinuous transmission mode (DCM). A DCM waveform is illustrated in Figure 3.

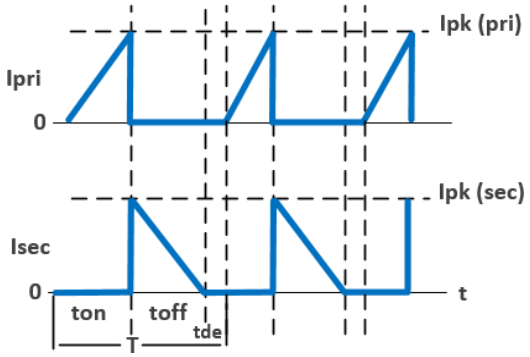

Figure 3. Discontinuous current mode (DCM) flyback current waveforms

In forward mode DC-DC converters, forward transformers are utilized for circuit isolation and voltage conversion. In forward transformers, the core isn't employed for energy storage. When the switch is turned, both the primary and secondary transmit at the same time, and the energy is processed straight through the transformer.

One of the first switching topologies is the push-pull transformer. With a single input, this transformer can produce numerous outputs. When the transformer's winding turn ratio is changed, the output voltages might be greater or lesser than the input voltages. Therefore, a push-pull converter is one in which currents are constantly pushed into and drawn from something. This is also a type of flyback transformer or an inductor. Current is constantly pushed and drawn from the transformer. With this push-pull method, the transformer transfers flux from the primary coil to the secondary coil, providing a kind of isolated voltage.

2.2. Electromagnetic Analysis via ANSYS/Maxwell

The ANSYS/Maxwell software tackles electromagnetic field issues across a substantial spatial domain by employing Maxwell's equations, considering user-defined starting conditions within suitable boundary parameters. It utilizes the finite element method (FEM) to address electrical or magnetic field challenges, employing various design and solver types tailored to specific equations. The analysis involves creating a mesh of basic units for the model, with the meshing process requiring careful parameter input to ensure optimal analysis outcomes. Overly complex meshes can lead to prolonged analysis times and potential computational capacity constraints, while overly simplified meshes may compromise analysis sensitivity. Correctly identifying current excitation in analyses involving electrical currents can pose challenges for many users. This study aims to address such challenges and highlight key considerations for ANSYS/Maxwell usage through a step-by-step analysis example utilizing a magnetostatic solver.

Depending on the choice of the class included in the program, the appropriate equation sets and terms are solved. There are three different design types (design types) available in ANSYS/Maxwell.

2.3. Mathematical Modeling

The mathematical model is realized for isolated discontinuous current flyback high-frequency transformer. First, it is necessary to consider some parameters which are already chosen. These parameters can be chosen according to the suitable usage area for any power application. Table 1 present the proposed HF transformer parameter to use for a HF step-down dc-dc converter.

Table 1. A 50/12.5/25 V single-phase flyback high-frequency transformer defined parameters

Symbols	Parameters	Units	Values
$V_{in\text{-}min}$	Minimum Input Voltage	V	50
$V_{in\text{-}max}$	Maximum Input Voltage	V	75
$V_{in\text{-}nominal}$	Nominal Input Voltage	V	12.5
V_{O1}	Output voltage 1	V	12.5
I_{O1}	Output Current 1	amps	2
V_{O2}	Output voltage 2	V	25
V_{O2}	Output Current 2	amps	0.5
K_u	Window Utilization	-	0.29
f	Frequency	kHz	20
R_{eq}	Equivalent Resistance	Ω	1
D_{max}	Max Duty Ratio	amps	0.5
D_w	Dwell Time Duty Ratio	watts	0.1
α	Regulation	%	1
B_m	Operating Flux Density	Tesla	0.3

American Wire Gauge (AWG) size and feature standard contain frequency values. By looking at the corresponding AWG according to the frequency value, certain parameters wire diameter, bare wire area, and resistance values are determined. The parameters are selected according to this standard. Table 2 presents the selected parameters.

Table 2. Selected wire parameters according to AWG standard

AWG	Selected wire size
Diameter (mm)	0.91186
Area (mm^2)	0.653
Resistance (ohm/km)	26.407
Max. current (A)	1.8
Max Frequency for 100% Skin Depth	21kHz
Bare Area ($10^{-3}cm^2$)	6.531

It has been chosen an ETD core with a core geometry that is comparable to core geometry (K_g). The core geometry for ETD ferrite cores as shown in Figure 4. Size and design data for ETD ferrite cores are given Table 3 and Table 4, respectively. EDT-39 is selected according to K_g parameters. It is the good option for choosing core type of high frequency flyback transformer.

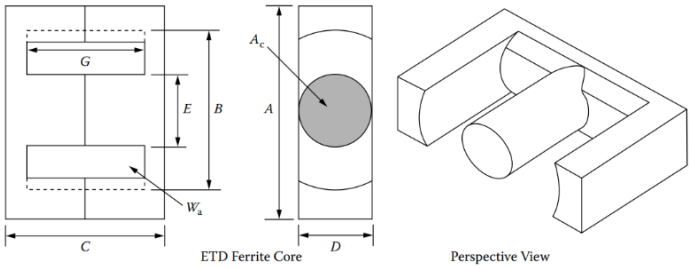

Figure 4. The core geometry for ETD ferrite cores [28]

An air gap put into the core has a strong demagnetizing impact, causing the hysteresis loop to "shearing over" and the permeability of high-permeability materials to drop significantly. Excitation by direct current maintains the same pattern. On the other hand, the introduction of a tiny air gap, has a much smaller impact on the core bias than on the magnetization properties. The amount of the air gap effect is affected by the length of the mean magnetic path and the uncut cores properties too. With a larger magnetic flux path, the drop in permeability is less apparent, but it is more noticeable in a large permeability core with a low coercive force.

A comparison of a common toroidal core B-H loop with and without a gap is shown in Figure 5. The gap expands the magnetic path's length. Due to highly inductive circuit, once the voltage E is impressed throughout a transformer's primary winding, the resultant current, will be minimal. Once the air gap is the smallest for a given core size, maximum inductance happens.

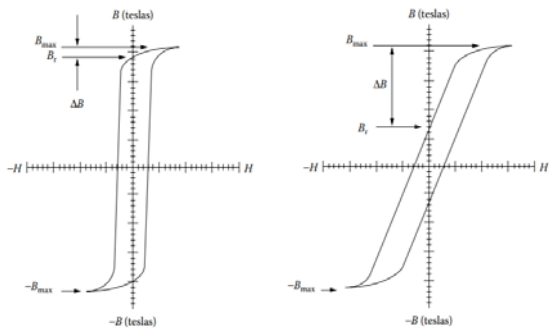

(a) (b)

Figure 5. Comparing magnetic materials a) with gap, b) without a gap [28]

Table 3. Size data for ETD ferrite cores

ETD, Ferrite Cores (Ferroxcube)						
Part No.	A (cm)	B (cm)	C (cm)	D (cm)	E (cm)	G (cm)
ETD-34	3.500	2.560	3.460	1.110	1.110	2.360
ETD-39	***4.000***	***2.930***	***3.960***	***1.280***	***1.280***	***2.840***
ETD-44	4.500	3.250	4.460	1.520	1.520	3.220

Table 4. Design data for ETD ferrite cores

ETD, Ferrite Cores (Ferroxcube)											
Part No.	W_{tcu} (grams)	W_{tfe} (grams)	MLT (cm)	MPL (cm)	$\frac{W_a}{A_c}$	A_c (cm^2)	W_a (cm^2)	A_p (cm^4)	K_g (cm^5)	A_t (cm^2)	*AL (mh/1K)
ETD-34	43.4	40.0	7.1	7.87	1.757	0.974	1.711	1.6665	0.0914	53.4	1182
ETD-39	***69.3***	***60.0***	***8.3***	***9.22***	***1.871***	***1.252***	***2.343***	***2.9334***	***0.1770***	***69.9***	***1318***
ETD-44	93.2	94.0	9.4	10.30	1.599	1.742	2.785	4.8515	0.3596	87.9	1682

Input power is not entirely passed to the output load in high frequency transformers. The loss power, which consists mostly of core loss and copper loss, is the difference between input power Pin and output power Pout. The efficiency of a transformer serves as a standard for its performance. The overall loss will be the least and the efficiency will be the maximum when core loss is equal to copper loss. Transformer losses versus output load current are shown in Figure 6.

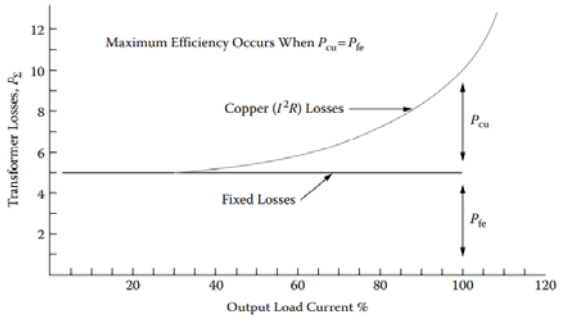

Figure 6. Transformer losses versus output load current [17]

The copper losses is exactly proportional to the properties of material. A design is influenced by a number of elements, size, material availability, temperature rise and cost. The use of iron alloys and ferrites in the construction of power inductors provides substantial advantages. The magnetic core material properties are given in Table 5. As can be seen in the Table 5, the effect of the material used on the flux density is compared. Ferrite was chosen as the most suitable material among the compared materials.

The mathematical model of the transformer yields the specifications for a 50/12.5/25 V flyback-type high-frequency transformer. Table 6 provides comprehensive details regarding the transformer's weight, electrical characteristics, and electromagnetic properties.

Table 5. Magnetic core material properties

Material name	**Composition**	**Initial permeability** μ_i	**Flux density** B_s	**Curie temperature** ℃	**Density grams/**cm^3 δ
Silicon	3-97 SiFe	1500	1.5-1.8	750	7.63
Orthonol	50-50 NiFe	2000	1.42-.158	500	8.24
Permalloy	80-20 NiFe	25000	0.66-0.82	460	8.73
Amorphous	81-3.5 FeSi	1500	1.5-1.6	370	7.32
Amorphous	66-4 CoFe	800	0.57	250	7.59
Amorphous (μ)	73-15 FeSi	30000	1.0-1.2	460	7.73
Ferrite	***MnZn***	***2500***	***0.5***	***>230***	***4.8***

Table 6. The design parameters of 50/12.5/25 V single-phase flyback-type high frequency transformer by using a mathematical model of the transformer

Symbols	Parameters	Units	Values
$\boldsymbol{\delta}$	Skin Depth	cm	0.0468
$\boldsymbol{D_{AWG}}$	Wire Diameter	cm	0.0936
$\boldsymbol{A_w}$	Base Wire Area	$m\Omega/cm$	263.9
T	Time Period	sec	$5 * 10^{-5}$
$\boldsymbol{t_{on}}$	Maximum Transistor on Time	sec	$2.5 * 10^{-5}$
$\boldsymbol{P_{o1}}$	Power out in secondary No.1	$watts$	27
$\boldsymbol{P_{o2}}$	Power out in secondary No.2	$watts$	13
$\boldsymbol{P_T\ or\ P_{omax}}$	Total Secondary Power	$watts$	40
$\boldsymbol{I_{pri,max}}$	Max Primary Current	$amps$	0.88
$\boldsymbol{I_{pri,pk}}$	Primary Peak Current	$amps$	3.55
$\boldsymbol{I_{pri_{RMS}}}$	Primary RMS Current	$amps$	1.45
$\boldsymbol{P_{in,max}}$	Maximum Input Power	$watts$	44.44
$\boldsymbol{R_{in,eq}}$	Equivalent Input Resistance	$ohms$	56.25
L	Primary Inductance	μH	351
W-S	Energy Handling Capability	$w-s$	0.0022
W-S	Energy Handling Capability	$w-s$	0.0022
$\boldsymbol{K_e}$	Electrical Condition	-	$5.22 * 10^{-5}$
$\boldsymbol{K_g}$	Core Geometry	cm^5	0.0946
J	Current Density	amps/cm^2	174.15
$\boldsymbol{A_{pw}(B)}$	Primary Wire Area	cm^2	$8.3 * 10^{-3}$
$\boldsymbol{S_{np}}$	The Required Number of Primary Strands	-	2
$\mathbf{N_p}$	The Number of Primary Turns	$turns$	26
$\boldsymbol{l_g}$	The Required Gap	cm	0.0266
mils	The Equivalent Gap in Mils	-	10.472
F	Fringing Flux Factor	-	1.1275
$\mathbf{N_{np}}$	The New Number of Turns N_{np}, by Inserting The Fringing Flux, F	$turns$	23
$\boldsymbol{B_{pk}}$	The Peak Flux Density	$teslas$	0.382
μΩ/cm	The primary, The new μΩ/cm	-	131.95
$\boldsymbol{P_p}$	Primary Copper Loss	$watts$	0.053
$\boldsymbol{N_{s01}}$	The Secondary Turns	turns	5
$\boldsymbol{I_{s01(pk)}}$	Secondary Peak Current	amps	10
$\boldsymbol{I_{s01(rms)}}$	The Secondary rms Current	amps	3.65
$\boldsymbol{A_{sw01(B)}}$	The Secondary Wire Area	cm^2	0.0210
$\boldsymbol{S_{ns01}}$	Required Number of Secondary Strands	-	3
$\boldsymbol{(S_{01})\mu\Omega/cm}$	The S_{01}secondary, μΩ/cm	-	82.2
$\boldsymbol{R_{s01}}$	The Winding Resistance	$ohms$	0.0037
$\boldsymbol{P_{s01}}$	The Secondary Copper Loss	$watts$	0.0487
$\boldsymbol{N_{s02}}$	The Secondary Turns	turns	10
$\boldsymbol{I_{s02(pk)}}$	The Secondary Peak Current	amps	2.5
$\boldsymbol{I_{s02(rms)}}$	The Secondary rms Current	amps	0.913
$\boldsymbol{A_{sw02(B)}}$	The Secondary Wire Area	cm^2	0.00524
$\boldsymbol{S_{ns02}}$	The Required Number of Secondary Strands	-	1
$\boldsymbol{(S_{02})\mu\Omega/cm}$	The, S_{02}, Secondary, μΩ/cm	-	263.9
$\boldsymbol{R_{S02}}$	The Winding Resistance	$ohms$	0.0219
$\boldsymbol{P_{s02}}$	The Secondary Copper Loss	$watts$	0.0183
$\boldsymbol{K_u}$	The Window Utilization	-	0.2086
$\boldsymbol{P_{cu}}$	The Total Copper Loss	$watts$	0.12
$\boldsymbol{\alpha}$	The Regulation, α, For this design	%	0.30
$\boldsymbol{R_p}$	Primary Winding Resistance	$ohms$	0.025
$\boldsymbol{B_{ac}}$	The AC Flux Density	$teslas$	0.191
WK	The Watts per Kilogram	watts/kg	12.4
$\boldsymbol{P_{fe}}$	The Core Loss	$watts$	0.7443
$\boldsymbol{P_\Sigma}$	The Total Loss, Core P_{fe} and Copper P_{cu}, in watts	$watts$	0.8643
$\boldsymbol{\Psi}$	The Watt Density	$watts/cm^2$	0.0124

3. ELECTROMAGNETIC ANALYSIS AND RESULTS

An analysis is conducted on a discontinuous high-frequency flyback transformer using electromagnetic methods. Initially, the transformer's characteristics are determined through a mathematical model, which includes losses (such as copper, core, and stray losses), transformer weight (including core and winding weights), and the dimensions of the core and windings. Subsequently, these parameters are optimized for weight and efficiency. Following optimization, the transformer is modeled in the ANSYS/Maxwell program, which is tailored for designing and analyzing electrical machines from an electromagnetic and thermal perspective. The design process for the transformer's core and windings will be elaborated upon in the subsequent steps. All the procedures are outlined below:

- Choosing the simulation type (electromagnetic, transient)
- Draw 3D the geometry
- Assign the materials
- Specify the boundary
- Assign the excitations and coil terminals
- Mesh operations
- Determine the solution setup
- Analyze Time Calculation
- Getting results and diagrams

The analysis of the high-frequency flyback transformer is conducted using the ANSYS/Maxwell simulation program in discontinuous mode. To accurately represent the transformer's electromagnetic nature, the solution type is selected as magnetic-transient, and the resulting analysis outcomes are time-dependent. The transformer's core and windings are then modelled using 3D-solid objects. Figure 7 displays the resulting model of the designed transformer.

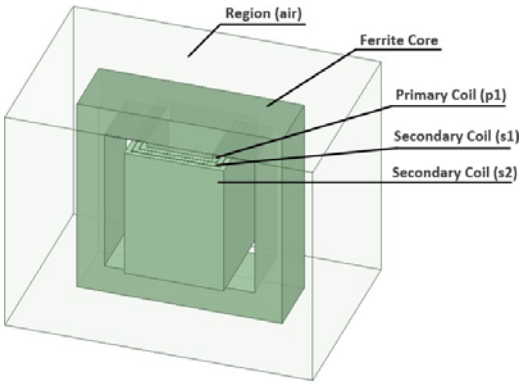

Figure 7. ANSYS Maxwell design of flyback high-frequency transformer

Following this, the transformer is structured in a 3D format, allowing for the design of its core, primary, and secondary windings utilizing Maxwell-3D, as illustrated in Figure 8.

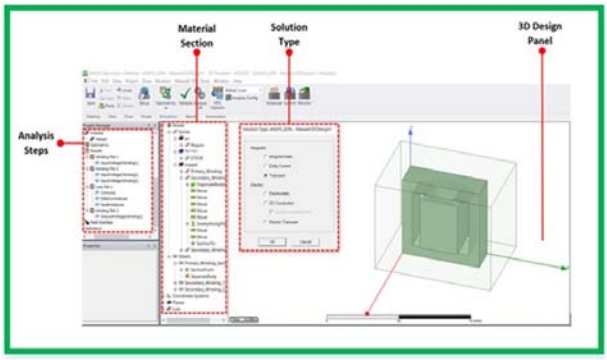

Figure 8. ANSYS/Maxwell 3D design operation panel

Once the transformer core and windings have been modeled, the material types for this equipment are chosen through the material property panel, as depicted in Figure 9.

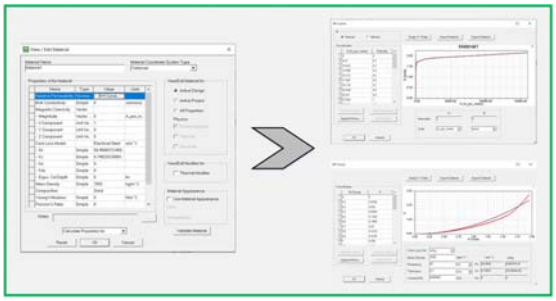

Figure 9. Creating specific material property and determining B-H and B-P curves of the core

During the design process, ferrite is specified as the core material for the transformer, with its characteristic features outlined in Section 2. Additionally, copper is chosen as the material for both the primary and secondary windings. Air material is then assigned to specific regions or boundaries due to the transformer's characteristics. After the assignment of materials, the primary and secondary windings are energised based on transformer parameters, taking into account factors such as turn ratio, ohmic resistance, and excitation terminal voltage values. The allocation of excitation to the windings is shown in Figure 10.

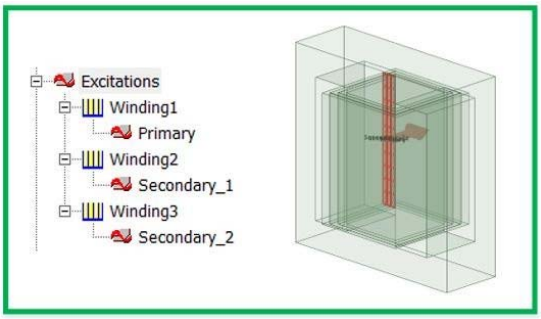

Figure 10. Assignment of excitation to the coil terminals of the transformer

The result of a finite element analysis (FEA) application should be independent of the mesh size. Convergence study not only accelerates the solution of the problem but also increases the accuracy of the result. Finite element analysis (FEA) is a method that can be used when making high-risk and costly decisions. Therefore, the finite element analysis results must be verifiable. To show the accuracy of the results, the mesh operation is used in the simulation study. The designed transformer undergoes a mesh operation, dividing it into 80000 particles, enabling electromagnetic analysis of each particle. This mesh operation enhances the accuracy of the analysis for the designed model. The mesh operation performed on the transformer model is illustrated in Figure 11.

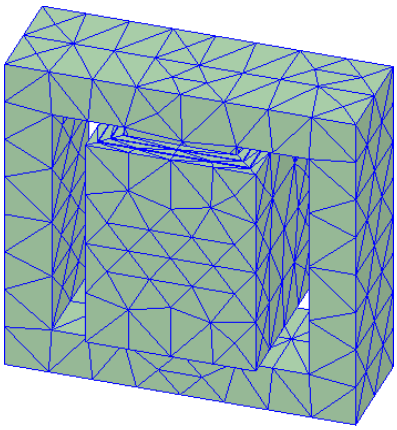

Figure 11. Mesh operation applied to the core and windings of the transformer

After completing these procedures, the transformer can be analyzed in subsequent stages. The analysis duration needs to be specified using the setup panel. The analysis solution step is employed in the setup panel to accurately define parameters such as type, start time, and stop time. These parameters are essential for achieving accurate electromagnetic transient analysis of the transformer as they directly affect the precision of the currents and voltages on the transformer. In this study, small ranges are selected for the analysis step size in order to obtain clear signals. The analysis configuration for the transformer is shown in Figure 12.

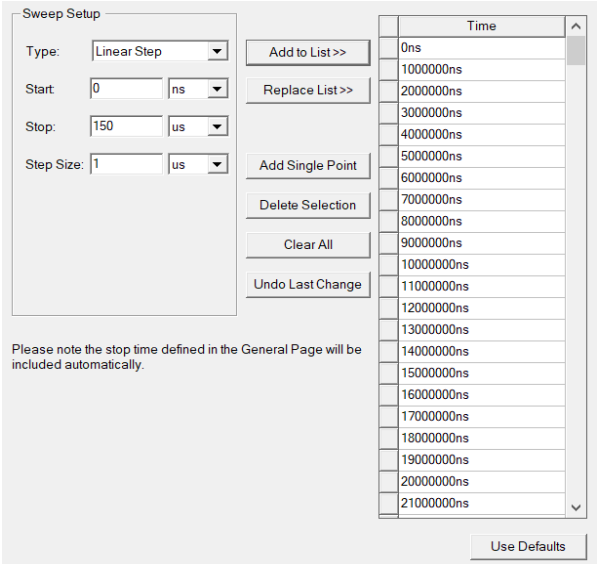

Figure 12. Analysis settings of the high-frequency transformer in ANSYS/Maxwell

The analysis duration ultimately determines the results. The electromagnetic transient analysis produces the following outcomes: When voltage is applied to the primary side of the coils, a varying magnetic field is generated within the transformer core and coils, resulting in voltage generation across the coil ends. The current and magnetic flux are both affected by changes in the magnetic field of the primary coil. This change in magnetic flux induces voltage in the secondary side of the coils. Figure 13 shows the analyzed transformer core and the distribution of magnetic flux.

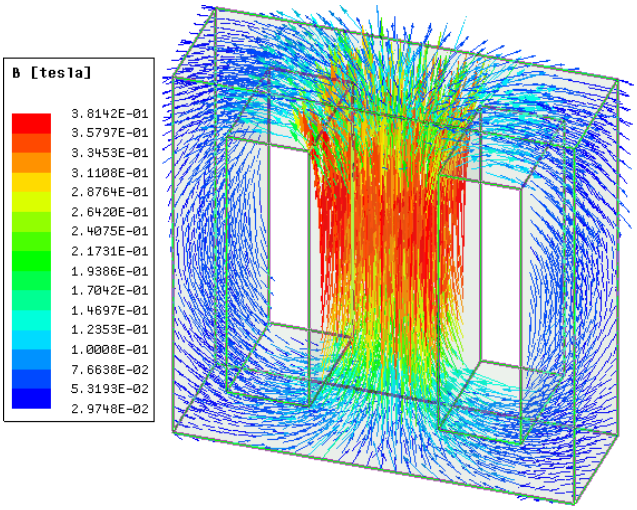

Figure 13. Magnetic field distribution on the transformer core

The transformer is subjected to testing in both normal load and overload scenarios. Under load, where 50 volts is supplied to the primary windings, 25 volts are induced in the secondary side. Figure 14 illustrates the primary and secondary voltages and currents of the engineered transformer.

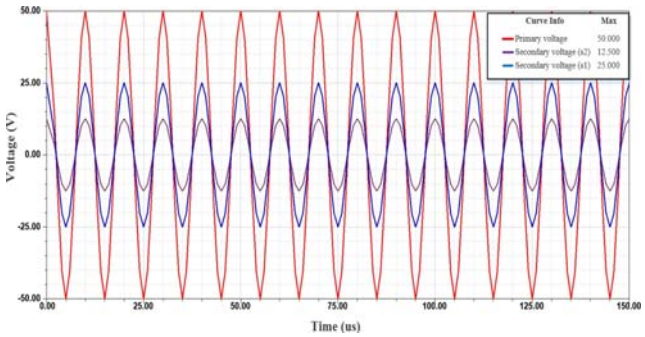

(a)

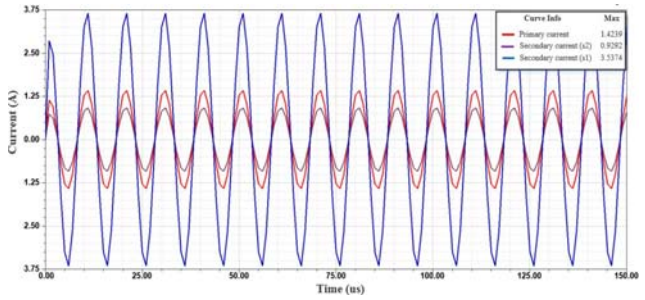

(b)

Figure 14. High-frequency flyback transformer primary and secondary (a) voltages (b) currents

Also, power loss analysis of the transformer is realized in the transformer core and coils. Figure 15. presents the power losses. When an alternating current flows through a coil wrapped around a core, it induces voltage in the core. This induced voltage leads to the creation of numerous closed-loop current paths within the core. This phenomenon occurs not only on the surface of the core but also within its interior. These currents, which form in the form of closed tiny rings, are called fuco currents (eddy currents). The current strength in each closed current path is directly proportional to the induced voltage. The current intensity is inversely proportional to the electrical resistance of this current path. Fuco currents cause overheating of the cores. Warming up means loss of energy. Some ferromagnetic materials, such as iron, become temporarily or permanently magnetic when exposed to an external magnetic field. This magnetism is opposite to the magnetic field on the transformer and causes energy loss as heat. This loss is called hysteresis loss. The hysteresis loss occurs in the form of heat as a result of the friction of the molecules with each other during the change of direction of the core molecules depending on the frequency. Copper loss is a term generally used for the heat produced by electric current in transformer windings or conductors of other electrical devices. All these losses in the HF transformer are presented with electromagnetic transient analysis results.

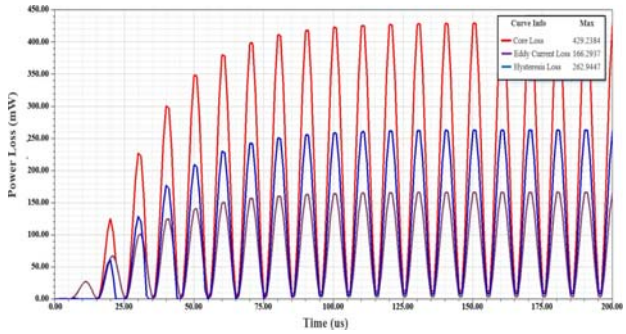

Figure 15. Power losses of the HF flyback transformer

When the losses in the HF transformer are examined, it is around 859 mW. In the mathematical model, it is seen that this power loss is about 864 mW. This shows that the simulation results are realistic. This realistic analysis is directly related to the transformer's core and coil selection, B-H and B-P characteristics, one-to-one dimension design and mesh operation. The HF transformer's total power is 40-W so the efficiency of the transformer is 97.8%.

4. CONCLUSIONS

The simple design of the high-frequency flyback transformer is smaller, lighter, and easier to install than other transformers. This means they are better suited to general electrical systems. A high-frequency flyback transformer usually has the same investment as other transformers. However, flyback converters, in which the high-frequency flyback transformer is the main component, are typically less expensive than similar converters because they consist of fewer components. An important benefit of the high-frequency flyback transformer is that it can be used as circuit isolation, which prevents electrical hazards and provides enhanced safety, especially for those near high-energy electrical systems. A high-frequency flyback transformer is used to isolate and switch multiple output voltages from a single control. A 50/12.5/25 V single-phase flyback transformer prioritizes optimal weight and size efficiency. Its parameters are derived through the utilization of a mathematical model. After performing the mathematical calculation, the transformer is designed using model parameters and then analyzed electromagnetically. The performance analysis of the HF transformer such as power losses, voltages, currents and magnetic field are verified with the experimental results. Thanks to this study, the efficiency and performance analysis of the HF transformer is performed before the transformer is produced. Also, the material selection of the HF transformer plays key role to achieve the great potential efficiency from the transformer. In the future study, CFD analyses of HF transformer and temperature and strength tests will be carried out under overload conditions. Also, the HF transformer will be experimentally exposed to the overload conditions and its strength and temperature analysis will be verified by simulation studies. Thus, before the HF transformer is produced commercially, both electromagnetic and temperature and strength tests will be carried out realistically.

5. REFERENCES

1. Elrajoubi, A.M., Ang, S.S., 2019. High-frequency transformer review and design for low-power solid-state transformer topology. 2019 IEEE Texas Power and Energy Conference (TPEC), 1-6.
2. Ding, H., Zhao, W., Li, M., Zhang, L., Sun, Y., 2023. Electromagnetic vibration characteristics of high-frequency transformer under DC bias with different winding structures. Processes, 11(4), 1185.
3. Yao, W., Lu, J., Taghizadeh, F., Bai, F., Seagar, A., 2023. Integration of SiC devices and high-frequency transformer for high-power renewable energy applications. Energies, 16(3), 1538.
4. Mukherjee, S., Barbosa, P., 2023. Design and optimization of an integrated resonant inductor with high-frequency transformer for wide gain range DC–DC resonant converters in electric vehicle charging applications. IEEE Transactions on Power Electronics, 38(5), 6380-6394.
5. Li, Z., Hsieh, E., Li, Q., Lee, F., 2023. High-frequency transformer design with medium-voltage insulation for resonant converter in solid-state transformer. IEEE Transactions on Power Electronics, 38(8), 9917-9932
6. Olowu, T.O., Jafari, H., Moghaddami, M., Sarwat, A.I., 2020. Multiphysics and multiobjective design optimization of high-frequency transformers for solid-state transformer applications. IEEE Transactions on Industry Applications, 57(1), 1014-1023.
7. Li, Z., Hsieh, Y.H., Li, Q., Lee, F.C., Ahmed, M.H., 2020. High-frequency transformer design with high-voltage insulation for modular power conversion from medium-voltage AC to 400-V DC. 2020 IEEE Energy Conversion Congress and Exposition (ECCE), 5053-5060.
8. Dang, Y., Zhu, L., Liu, J., Zhan, C., Long, L., Ji, S., 2022. Module integral method for the calculation of frequency-dependent leakage inductance of high-frequency transformers. IEEE Transactions on Power Electronics, 37(6), 7028-7038.
9. Rahman, S,, Candan, M.Y., Tamyurek, B., Aydin, E., Meşe, H., Aydemir, M.T., 2022. Design and implementation of a 10 kV/10 kW high-frequency center-tapped transformer. Electrical Engineering, 1-17.
10. Barg, S., Bertilsson, K., 2019. Multi-objective pareto and GAs nonlinear optimization approach for flyback transformer. Electrical Engineering, 101(3), 995-1006.
11. Ahmed, N.A., Madouh, J.Y., 2018. High-frequency full-bridge isolated DC–DC converter for fuel cell power generation systems. Electrical Engineering, 100(6), 1-13.
12. Guillod, T., Krismer, F., Kolar, J.W., 2018. Magnetic equivalent circuit of MF transformers: modeling and parameter uncertainties. Electrical Engineering, 100, 2261-2275.
13. Huang, P., Mao, C., Wang, D., 2017. Electric field simulations and analysis for high voltage high power medium frequency transformer. Energies, 10(3), 371.

14. Olowu, T.O., Jafari, H., Moghaddami, M., Sarwat, A.I., 2019. Physics-based design optimization of high frequency transformers for solid state transformer applications. 2019 IEEE Industry Applications Society Annual Meeting, 1-6.
15. Gradinger, T.B., Drofenik, U., Alvarez, S., 2017. Novel insulation concept for an MV dry-cast medium-frequency transformer. 2017 19th European Conference on Power Electronics and Applications (EPE'17 ECCE Europe), 1-10.
16. Kauder, T., Hameyer, K., 2017. Performance factor comparison of nanocrystalline, amorphous, and crystalline soft magnetic materials for medium-frequency applications. IEEE Transactions on Magnetics, 53(11), 1-4.
17. Kiran, M.R., Farrok, O., Islam, M.R., Zhu, J., 2021. Increase in the power transfer capability of advanced magnetic material based high frequency transformer by using a novel distributed winding topology. IEEE Transactions on Industry Applications, 57(6), 6306-6317.
18. Gao, Z., Zhang, J., Guo, F., Zhou, Y., Guan, R., Huang, Y., 2021. An improved high-voltage high-frequency multi-winding transformer structure for anode power supply in ECRH. Fusion Engineering and Design, 172, 112899.
19. Nia, M.S.S., Saadatmand, S., Altimania, M., Shamsi, P., Ferdowsi, M., 2019. Analysis of skin effect in high frequency isolation transformers. 2019 North American Power Symposium (NAPS), 1-6.
20. Islam, M.R., Rahman, M.A., Sarker, P.C., Muttaqi, K.M., Sutanto, D., 2019. Investigation of the magnetic response of a nanocrystalline high-frequency magnetic link with multi-input excitations. IEEE Transactions on Applied Superconductivity, 29(2), 1-5.
21. Nia, M.S.S., Saadatmand, S., Altimania, M., Shamsi, P., Ferdowsi, M., 2019. Analysis of various transformer structures for high frequency isolation applications. 2019 North American Power Symposium (NAPS), 1-6.
22. Zhao, B., Ouyang, Z., Andersen, M.A.E., Duffy, M.C., Hurley, W.G., 2017. An improved partially interleaved transformer structure for high-voltage high-frequency multiple-output applications. Proceedings of IEEE 43rd Annual Conference of IEEE Industrial Electronics, 798-804.
23. Guo, S., Liu, P., Zhang, L., Huang, A.Q., 2017. Design and optimization of the high frequency transformer for a 800V/1.2 MHz SiC LLC resonant converter. 2017 IEEE Energy Conversion Congress and Exposition (ECCE), 5317-5323.
24. Mogorovic, M., Dujic, D., 2018. Sensitivity analysis of medium-frequency transformer designs for solid-state transformers. IEEE Transactions on Power Electronics, 34(9), 8356-8367.
25. Chen, T., Zhao, Z., Shen, Z., Jia, H., Ji, J., Wang, H., 2024. Litz-wire winding loss calculation method for optimal design of high-frequency transformers. IEEE Journal of Emerging and Selected Topics in Power Electronics, 12(2), 2027-2040.
26. Rajput, N., Sandhibigraha, H.B., Mahadeva Iyer, V., 2024. Analysis and design trade-offs of a multi-winding high-frequency transformer for a battery charger. 2024 IEEE Applied Power Electronics Conference and Exposition (APEC), 854-860.
27. Nasirpour, F., Heidary, A., Niasar, M.G., Lekić, A., Popov, M., 2023. High-frequency transformer winding model with adequate protection. Electric Power Systems Research, 223, 109637.
28. Colonel, W.T., 2011. Transformer and inductor design handbook. 4th ed; CRC Press: Boca Raton, FL, USA.